 CMES, vol.10, no.1, pp.13-38, 2005

A Group Preserving Scheme for Inverse Heat Conduction Problems

C.-W. Chang[1], C.-S. Liu[2] and J.-R. Chang[1,3]

Abstract: In this paper, the inverse heat conduction problem governed by sideways heat equation is investigated numerically. The problem is ill-posed because the solution, if it exists, does not depend continuously on the data. To begin with, this ill-posed problem is analyzed by considering the stability of the semi-discretization numerical schemes. Then the resulting ordinary differential equations at the discretized times are numerically integrated towards the spatial direction by the group preserving scheme, and the stable range of the index $r = 1/2\nu\Delta t$ is investigated. When the numerical results are compared with exact solutions, it is found that they are in a good agreement even under noisy data. It is also shown that the group preserving scheme is quite effective and better than other numerical solvers, including the fourth-order Runge-Kutta method.

keyword: Inverse heat conduction problem, group preserving scheme, ill-posed problem, semi-discretization

1 Introduction

Inverse problems are presently becoming more and more important in many fields of science and engineering and they typically result in mathematical models that are not well-posed in the sense of Hadamard (1953), referring also Maz'ya and Shaposhnikova (1998). In other words, it means that one or more of the following properties does not hold: for all admissible data, a solution exists; for all admissible data, the solution is unique; the solution depends continuously on the data. Problems that fail to meet these prerequisites are said to be ill-posed.

Over the last few decades, much interest has been directed towards the employment of inverse techniques for solving different engineering problems that cannot be depicted mathematically by direct methods. This situation transpires when all the required data to solve a direct problem or to procure a trustworthy direct solution is not available. Inverse problem can be defined as a problem where all results are found when a part of them is known and some boundaries or reasons may linger unknown. Such a problem is much more difficult to solve than a direct one. The reason for this is that it is usually ill-posed and very sensitive to the measurement errors. The problem is often encountered in the field of heat conduction and referred to as the inverse heat conduction problem (IHCP); see, e.g., Beck, Blackwell and Clair (1985). We will refer to it as the sideways heat equation in order to discriminate it from other inverse problems for the parabolic type partial differential equations.

Many finite difference discretizations for the sideways heat equation are discussed in Beck and Blackwell (1985), and many are interpreted and compared by Carasso (1992, 1993). Besides, stability standpoints of those finite difference algorithms in connection with mollification are contemplated in a series of papers; see, e.g., Murio (1989), Guo, Murio and Roth (1990), Murio and Guo (1990), Guo and Murio (1991), and Al-Khalidy (1998a). In these successful computations with the space-marching, finite difference methods are also described. For instance, Eldén (1995a, 1995b) discretized the sideways heat equation by a differential-difference equation and analyzed the approximation properties of time-discrete approximations by using the Fourier transform techniques. He mentioned that the time discretization has a "regularizing effect", that is, the high-frequency noise is prevented from blowing up. Moreover, Krutz, Schoenhals and Hore (1978), Lithouhi and Beck (1986), and Reinhardt (1991) employed a finite element method (FEM) to solve the IHCP. Drawbacks of applying finite differences and finite elements are that they usually produce instabilities in the numerical schemes and require a large number of cells or elements.

The boundary element method (BEM) has been considered in the study of IHCP and utilized by many researchers. Brebbia (1984) first employed the BEM to

[1] Department of Systems Engineering and Naval Architecture, National Taiwan Ocean University, Keelung 20224, Taiwan
[2] Department of Mechanical and Mechatronic Engineering, National Taiwan Ocean University, Keelung 20224, Taiwan
[3] * Corresponding author, Tel.: +886-2-24622192x6031; fax: +886-2-24625945; E-mail address: cjr@mail.ntou.edu.tw (J.R. Chang)

avoid the additional finite differencing required in the conventional FEM for heat transfer problems. Since then, several researchers have begun to use various BEM formulations to treat the ill-posed problem existing in this field; see, e.g., Le Niliot , Papini and Pasquetti (1990), Ingham, Yuan and Han (1991), Pasquetti and Le Niliot (1991), Kurpisz and Nowak (1992, 1995), Yuan (1993), and Ingham and Yuan (1994). After that, Lesnic, Elliott and Ingham (1996) used the BEM along with the minimum energy technique to solve the IHCP, namely to determine the temperature and heat flux on the remaining boundary. Besides, Lesnic, Elliott and Ingham (1998) also extended the results of Cannon (1963) for solving the IHCP when no boundary condition is prescribed and used the BEM to find the solution numerically. In addition, Al-Najem, Osman, El-Refaee and Khanafer (1998) employed the singular value decomposition (SVD) with BEM and the least-squares approach with integral transform method to deal with two-dimensional steady-state IHCPs. Shen (1999) even employed two BEMs, a collocation method and a weighted one, to solve the IHCP. Moreover, Singh and Tanaka (2001) also presented an application of the dual reciprocity boundary element method (DRBEM) in conjunction with iterative regularization for the solution of time-dependent IHCPs. Based on the dual reciprocity boundary element along with sequential function specification scheme, Behbahani-nia and Kowsary (2004) have recently proposed a method to deal with two-dimensional IHCPs involving unknown time and space varying boundary heat flux estimation. Since there is no need on domain discretization in the BEM, the location of interior points, in which the temperature data are gathered, can be selected in a rather arbitrary way; see, e.g., Chantasiriwan (2001). It should be noted that Ochiai and Sladek (2004) have recently proposed a numerical treatment of domain integrals in three-dimensional boundary integral formulations which is without the need to discretize the interior of the domain especially for thermal stress analysis with arbitrary internal heat generation. Comparing with those mesh-dependent methods like FEM and BEM, the meshless methods [e.g., Hon and Wei (2002, 2005)], which do not require any domain or boundary discretization, have been proposed. In general, applications of the BEM in this field decreases the computational time and capacity requirement but the problem of numerical stability still exists.

The IHCP in thermodynamics is also treated by different workers in computational thermodynamics with various numerical schemes. For example, the wavelets method [e.g., Liu, Guerrier and Benard (1995), Reginska (1995, 2001), Fu, Qiu and Zhu (2002, 2003), Reginska and Eldén (1997, 2000), Eldén, Berntsson and Reginska (2000), and Qiu, Fu and Zhu (2003)], the method of quasi-reversibility [e.g., Blanc, Raynaud and Chau (1998)] and the Fourier analysis [e.g., Seidman and Eldén (1990), Prud'homme and Nguyen (1999), and Berntsson (2003)] have been adopted for solving the ill-posed sideways heat equation. Besides, Dorai and Tortorelli (1997) employed the Newton's method, which is superior to the first-order variable metric method due to its limited dependence on regularization and faster convergence, to solve the IHCP. In addition, Eldén (1997) and Berntsson (1999) used time differencing combined with a "method of lines" for solving numerically the initial value problem in the space variable. This approach was proposed as an alternative way of implementing space-marching methods for the sideways heat equation. Examples of this are also found in the works of Al-Khalidy (1998b). Besides, Taler and Zima (1999) have used the control volume algorithm to solve IHCP and Blanc, Raynaud and Chau (1998) also provided a step by step guide to facilitate the use of the function specification method for 2D IHCPs. Furthermore, an iterative approach [e.g., Yang (1999a)], the sequential method [e.g., Yang (1999b), Chantasiriwan (1999), Battaglia, Cois, Puigsegur and Oustaloup (2001), and Liu, Chen and Yang (2004)] and the approximate inverse method [e.g., Jonas and Louis (1999)] were developed for reconstructing the solutions of IHCPs.

In respect of regularization, the use of a reduced model for the solution of IHCP was introduced by Videcoq and Petit (2001). The method includes the regularization with the function specification technique, which gives accurate results. Besides, the application of Alifanov's iterative regularization method [e.g., Su and Neto (2001)] to estimate infinite-dimensional quantities in IHCPs is also found. As for the remedy in a hybrid numerical algorithm for IHCPs, the Laplace transform technique and the finite difference method with a sequential-in-time concept and the least-square scheme [e.g., Chen, Lin and Fang (2001), Chen, Lin and Wang (2002)] were proposed to predict the unknown surface temperature in two-dimensional IHCPs. In addition, the Laplace transform technique and control volume method in conjunc-

tion with the hyperbolic shape function and least-square scheme [e.g., Chen, Peng, Yang and Fang (2001)] were applied to estimate unknown surface conditions of one-dimensional hyperbolic IHCPs. Also, the model reduction method with singular decomposition [e.g., Kim and Lee (2002)] provides an efficient numerical method for solving IHCPs. Based on the decomposition of the thermal field on the modal basis constituted by the set of eigenvalues and eigenfunctions of the heat diffusion operator, a modal approach [e.g., Battaglia (2002)] has recently been proposed. With the Lagrange theory for dynamic optimization and model size reduction technique, Palomo (2003) also successfully solved the multidimensional IHCPs. Recently, a numerical procedure using a combined differential quadrature and Taylor series approach [e.g., O'Mahoney (2003)] and an analytical method using the Laplace transform technique [e.g., Monde, Arima, Liu, Mitutake and Hammad (2003)] have been presented for solutions of the two-dimensional transient IHCPs. A fundamental solution method with mesh-free technique categorized into BEM [e.g., Hon and Wei (2004)] for IHCP is specially noticed in the BEM community. Moreover, a transfer function, based on Duhamel integral [e.g., Lahoucine (2004)], was proposed and the measured response was approximated by a quasi-periodic function. Furthermore, the Bayesian inference approach providing a solution to IHCP by formulating a complete probabilistic description of the unknown and uncertainties given temperature data was also reported [e.g., Wang and Zabaras (2004, 2005)]. However, to our best knowledge, Eldén (1995a) only considered discretization in time for solving the IHCP and this may arise from the ill-posedness and numerical instability of the problem.

In this paper, we propose a new numerical scheme for solving the sideways heat equation. Based on the numerical method of line, which is also a well-developed numerical method, the proposed scheme can transform the partial differential equation into a system of ordinary differential equations. The major contributions made in this paper are the applying of group preserving property of the resultant system in developing an effective numerical scheme and giving a persuasion that the proposed scheme is superior to the Euler scheme and the fourth-order Runge-Kutta method even it requires calculating an adaptive factor. More importantly, the proposed scheme is easy to implement and time saving. Through this study, we can have an easy-implementation and explicit-single step group preserving scheme (GPS) used in the calculations of the sideways heat equation. The accuracy of the proposed scheme is much better than the Euler scheme, and it may over the fourth-order Runge-Kutta method.

2 Inverse problem statement

In many industrial applications we may want to determine the temperature on the surface of a body, but the surface itself is inaccessible for a measurement. It may also be the case that locating a measurement device on the surface would disturb the measurements so that an incorrect temperature is recorded. In such cases one is restricted to internal measurements. Berntsson (2003) has presented an example of an industrial application where the sideways heat equation can be used. He has considered a particle board, on which a thin lacquer coating is to be applied. In order to reduce the time for the lacquer coating to dry, we initially heat the particle board. Since the temperature gradients on and close to the surface of the board influence the drying time and the quality of the lacquer coating, it is important to estimate the temperature and the temperature gradients on the surface of the board. It is usually difficult or impossible to measure the temperature directly on the surface of the board, instead, we can drill a hole from the other side of the board and place a thermocouple close to the surface to measure the temperature.

The sideways heat equation is a model of a situation that when the temperature data from a measurement device located inside a body is available, we attempt to decide the outside temperature of the body. Here we are concerned with the numerical solutions of

$$u_t = \nu u_{xx},\ l \geq x \geq 0, t \geq 0, \tag{1}$$

with a left-side boundary condition:

$$u(0,t) = \alpha(t),\ t \geq 0, \tag{2}$$

and initial condition:

$$u(x,0) = h(x),\ l \geq x \geq 0, \tag{3}$$

in which ν is the thermal conductivity of a heat-conducting rod with length l.

When it is impossible to measure the temperature on the surface directly, the sideways heat equation often occurs in engineering appliances, in which one wants to resolve the surface temperature from measurements inside a heat-conducting object. The problem setup with its physical model is shown in Fig. 1. Suppose that we can insert a thermocouple inside the rod to measure the temperature at a position $x = a < l$, and the data is denoted by

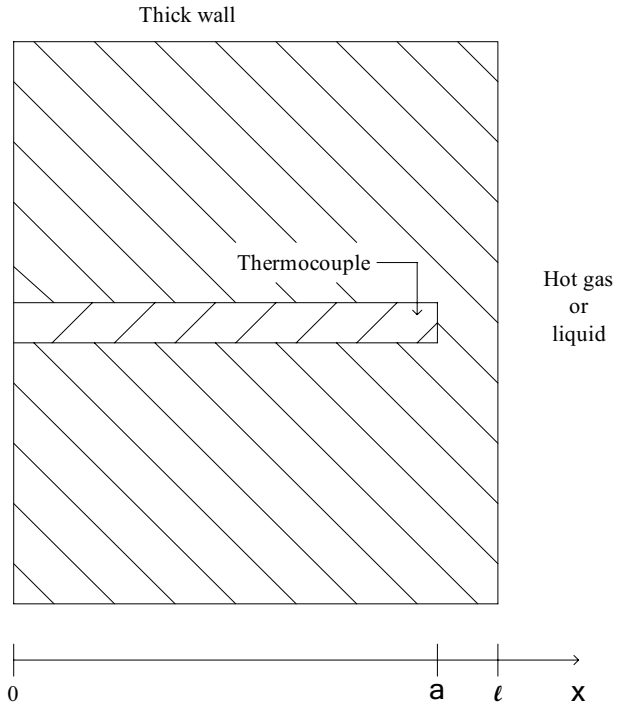

Figure 1 : Determination of surface temperature from interior measurements. The thermocouple could be superseded by any thermal sensor.

$$u(a,t) = \beta(t),\ t \geq 0. \tag{4}$$

The inverse problem is thus to decide the temperature field inside the rod by using Eqs. (1)-(4).

When we want to recover the temperature on the other side at $x = l$, we can use the solution of the above problem. However, this problem is ill-posed in the sense that the solution does not depend continuously on the data given or measured. Therefore, we first transform Eq. (1) to the following equations:

$$\frac{\partial u(x,\ t)}{\partial x} = v(x,\ t),$$

$$\frac{\partial v(x,\ t)}{\partial x} = \frac{\partial u(x,\ t)}{\nu \partial t}.$$

Then, by using a semi-discretized method to discretize the quantities of $u(x,t)$ and $v(x,t)$ along the time direction, we can obtain a system of ordinary differential equations for u and v with x as independent variable. In order to integrate these differential equations, let us first briefly sketch the so-called group-preserving scheme developed by Liu (2001) for ordinary differential equations in the next section.

3 The group preserving schemes

Consider a system of n ordinary differential equations:

$$\mathbf{u}' = \mathbf{f}(\mathbf{u},x),\ \mathbf{u} \in R^n,\ x \in R, \tag{5}$$

where $\mathbf{u}$ is an n-dimensional unknown vector, x is a space variable, and $\mathbf{f}$ is a vector-valued function of $\mathbf{u}$ and x. The prime stands for the differential with respect to x. For the uniqueness of the solution, the Lipschitz condition is assumed

$$\|\mathbf{f}(\mathbf{u},x) - \mathbf{f}(\mathbf{y},x)\| \leq L\|\mathbf{u}-\mathbf{y}\|,\ \forall (\mathbf{u},x),(\mathbf{y},x) \in D, \tag{6}$$

where D is a domain in $R^n \times R$, and L is known as a Lipschitz constant.

Liu (2001) has rewritten Eq. (5) into the following form

$$\frac{d}{dx}\begin{bmatrix} \mathbf{u} \\ \|\mathbf{u}\| \end{bmatrix} = \begin{bmatrix} 0_{n\times n} & \frac{\mathbf{f}(\mathbf{u},x)}{\|\mathbf{u}\|} \\ \frac{[\mathbf{f}(\mathbf{u},x)]^t}{\|\mathbf{u}\|} & 0 \end{bmatrix} \begin{bmatrix} \mathbf{u} \\ \|\mathbf{u}\| \end{bmatrix} \tag{7}$$

if $\|\mathbf{u}\| > 0$. Here, $\|\mathbf{u}\|$ stands for the Euclidean norm of $\mathbf{u}$, and the superscript 't' denotes the transpose. It is obvious that the first equation is the same as the original Eq. (5), but the introduction of the second equation leads to a Minkowskian structure for the augmented nonlinear system with the augmented variables $\mathbf{X} = (\mathbf{u}^t, \|\mathbf{u}\|)^t$ satisfying

$$\mathbf{X}^t\mathbf{g}\mathbf{X} = 0, \tag{8}$$

where

$$\mathbf{g} = \begin{bmatrix} I_n & 0_{n\times 1} \\ 0_{1\times n} & -1 \end{bmatrix} \tag{9}$$

is a Minkowski metric, and I_n is the identity matrix of order n. For this form of $\mathbf{X}' = \mathbf{A}\mathbf{X}$, the augmented matrix $\mathbf{A}$ is given by

$$\mathbf{A} = \begin{bmatrix} 0_{n\times n} & \frac{\mathbf{f}(\mathbf{u},x)}{\|\mathbf{u}\|} \\ \frac{[\mathbf{f}(\mathbf{u},x)]^t}{\|\mathbf{u}\|} & 0 \end{bmatrix}, \tag{10}$$

and satisfies

$$\mathbf{A}^t\mathbf{g} + \mathbf{g}\mathbf{A} = \mathbf{0}, \tag{11}$$

which shows that $\mathbf{A}$ is a Lie algebra of the Lorentz group $SO_o(n,1)$.

Remarkably, the original n-dimensional Eq. (5) in R^n can be embedded naturally into an augmented n+1-dimensional Eq. (7) in M^{n+1}, satisfying the cone condition:

$$\mathbf{X}^t\mathbf{g}\mathbf{X} = \mathbf{u}\cdot\mathbf{u} - \|\mathbf{u}\|^2 = \|\mathbf{u}\|^2 - \|\mathbf{u}\|^2 = 0, \tag{12}$$

which is the most natural constraint that we can impose on Eq. (5). Even raising the dimension of the new system by one, it shows that the new system with its Lie algebra property in Eq. (11) has the advantage of allowing us to develop the group preserving numerical scheme [Liu (2001, 2004)]:

$$\mathbf{u}_{i+1} = \mathbf{u}_i + \frac{4\Delta x\|\mathbf{u}_i\|^2 + 2(\Delta x)^2\mathbf{f}_i\cdot\mathbf{u}_i}{4\|\mathbf{u}_i\|^2 - (\Delta x)^2\|\mathbf{f}_i\|^2}\mathbf{f}_i. \tag{13}$$

The numerical formula of Eq. (13), which upon comparing with the Euler scheme

$$\mathbf{u}_{i+1} = \mathbf{u}_i + \Delta x\,\mathbf{f}_i, \tag{14}$$

can be viewed as a weighting factor adaptive numerical scheme:

$$\mathbf{u}_{i+1} = \mathbf{u}_i + \eta_i\Delta x\,\mathbf{f}_i \tag{15}$$

with the adaptive factor

$$\eta_i = \frac{4\|\mathbf{u}_i\|^2 + 2\Delta x\,\mathbf{f}_i\cdot\mathbf{u}_i}{4\|\mathbf{u}_i\|^2 - (\Delta x)^2\|\mathbf{f}_i\|^2} \tag{16}$$

changing step-by-step. In the above equations, $\mathbf{u}_i$ denotes the numerical value of $\mathbf{u}$ at a discrete spatial point x_i, $\Delta x = x_{i+1} - x_i$ is a uniform spatial increment, and $\mathbf{f}_i$ denotes $\mathbf{f}(\mathbf{u}_i, x_i)$.

4 The inverse heat conduction problems

4.1 Semi-discretization

The numerical method of line is simple in concept that for a given system of partial differential equations one discretizes all but one of the independent variables. The semi-discrete procedure yields a coupled system of ordinary differential equations, which are then numerically integrated. For the one-dimensional heat flow equation, we adopt the numerical method of line to discretize the time coordinate t by

$$\begin{aligned} &\frac{\partial u^i(x)}{\partial x} = v^i(x),\ i = 1,\ldots,n, \\ &\frac{\partial v^i(x)}{\partial x} = \frac{u^{i+1}(x) - u^{i-1}(x)}{2\nu\Delta t},\ i = 1,\ldots,n-1, \\ &\frac{\partial v^n(x)}{\partial x} = \frac{u^n(x) - u^{n-1}(x)}{\nu\Delta t}, \end{aligned} \tag{17}$$

where u is a scalar temperature field of heat distribution, Δt is a uniform discretization time increment, which together with v can be viewed as parameters of the above differential equations and $u^i(x) = u(x, i\Delta t)$. Eq. (17) can be expressed by Eq. (5) as a vector form with $\mathbf{u} = (u^1,\ldots,u^n,v^1,\ldots,v^n)^t$ and $f = (v^1,\ldots,v^n,(u^2 - u^0)/(2\nu\Delta t),\ldots,(u^{n-1} - u^{n-2})/(2\nu\Delta t),(u^n -$

$u^{n-1})/(\nu\Delta t))^t$.

The next step is to advance the solution from the boundary condition at x = 0 to the end boundary at $x = l$. Really,

Eq. (17) has totally $2n$ coupled linear differential equations for the $2n$ variables $u^i(x)$ and $v^i(x)$, $i=1,\ 2,\ldots,n$, which can be numerically integrated to obtain the solutions. When $i=0$, $u^0(x)=h(x)$ can be obtained from Eq. (3). The formulation of the above problem is schematically shown in Fig. 2, where x is an integration direction.

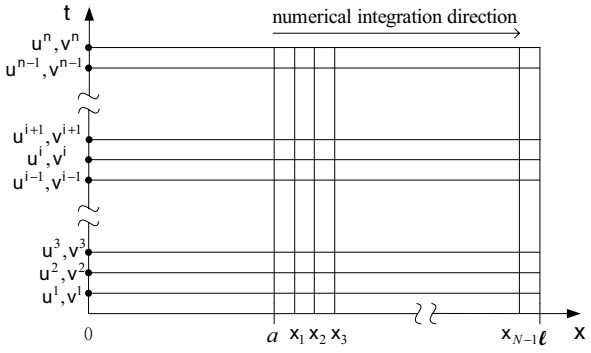

Figure 2 : The discretization of sideways heat equation.

Suppose that

$$\frac{\partial u^i(x)}{\partial x}\Big|_{x=j\Delta x}=\frac{u^i((j+1)\Delta x)-u^i(j\Delta x)}{\Delta x},$$

$$\frac{\partial v^i(x)}{\partial x}\Big|_{x=j\Delta x}=\frac{v^i((j+1)\Delta x)-v^i(j\Delta x)}{\Delta x}$$

by a forward difference for the partial derivatives of u and v with respect to x, and for saving notation we let

$$\begin{aligned} u^i_j &= u(a+j\Delta x,\ i\Delta t),\\ v^i_j &= v(a+j\Delta x,\ i\Delta t), \end{aligned} \tag{18}$$

and let

$$r=\frac{1}{2\nu\Delta t} \tag{19}$$

be the stability index, then we can fully discretize the sideways heat equation (17) into the following form:

$$u^i_{j+1}=u^i_j+v^i_j\Delta x,\ j=0,1,\ldots,N,\ i=1,\ldots,n,$$

$$\begin{aligned} v^i_{j+1} &= v^i_j+r\Delta x(u^{i+1}_j-u^{i-1}_j),\\ &\quad j=0,1,\ldots,N,\ i=1,\ldots,n-1 \end{aligned} \tag{20}$$

$$v^n_{j+1}=v^n_j+2r\Delta x(u^n_j-u^{n-1}_j),$$

where N is the number of spatial steps and such that $\Delta x=(l-a)/N$, and a is the distance of the thermocouple with $0\le a<l$. At this moment let us return to Eqs. (1)-(4), where the problem in the ranges of $0\le x\le a$ and $t\ge 0$ is well-defined to be a Cauchy type PDE. By applying the elementary method to this problem, we are easy to derive $u(x,t)$ and thus, $v(x,\ t)=\partial u(x,\ t)/\partial x$ available in the above ranges. Therefore, the data of u^i_0 and v^i_0 required in our numerical integrations are available, and all u^i_0 and v^i_0 , $i=1,\ldots,n$, are known.

We can step the solutions u^i_{j+1} and v^i_{j+1} according to Eq. (20), since all the terms on the right-hand sides are already known at the previous spatial step. If the ratio $r\Delta x$ is chosen smaller, there will be improved accuracy. If the ratio $r\Delta x$ is chosen greater, the number of calculations required to advance the solution through a given spatial interval would decrease. Nevertheless, for the numerical scheme of Eq. (18) there is no such freedom to select larger $r\Delta x$, because when $r\Delta x$ is larger the instability causes the scheme to fail in calculating the heat responses; see, e.g., Richtmyer (1967).

4.2 Group preserving scheme

In addition to the explicit scheme of the Euler type introduced in the previous subsection, we attempt to develop another explicit scheme for the heat flow equation according to the formalism specified in Section 3. From Eq. (17) we have an ordinary differential equations system for the 2n unknowns of $u^i(x)$ and $v^i(x)$, $i=1,2,\ldots,n$. By employing the numerical scheme developed in Section 3 to Eq. (17), we have

$$\begin{aligned} u^i_{j+1} &= u^i_j+\eta_j\Delta x v^i_j,\ j=0,1,\ldots,N,\ i=1,\ldots,n,\\ v^i_{j+1} &= v^i_j+\eta_j r\Delta x(u^{i+1}_j-u^{i-1}_j),\\ &\quad j=0,1,\ldots,N,\ i=1,\ldots,n-1,\\ v^n_{j+1} &= v^n_j+2\eta_j r\Delta x(u^n_j-u^{n-1}_j). \end{aligned} \tag{21}$$

We can easily realize the scheme as shown in Fig. 2. If $\eta_j=1$ for each step of x_j, then the above scheme is reduced to the Euler scheme of Eq. (20).

4.3 Stability analysis

We proceed to investigate the stability of scheme in Eq. (21), which can be expressed by a matrix equation

$$\begin{bmatrix} u^1_{j+1} \\ v^1_{j+1} \\ u^2_{j+1} \\ v^2_{j+1} \\ \cdot \\ \cdot \\ \cdot \\ \cdot \\ u^n_{j+1} \\ v^n_{j+1} \end{bmatrix} = \begin{bmatrix} 1 & \eta_j\Delta x & & & & & & & & \\ & 1 & r\eta_j\Delta x & & & & & & & \\ & & 1 & \eta_j\Delta x & & & & & & \\ -r\eta_j\Delta x & & & 1 & r\eta_j\Delta x & & & & & \\ & & & & \cdot & & & & & \\ & & \cdot & & & & & & & \\ & & & & \cdot & & & & & \\ & & & & & \cdot & & & & \\ & & & & & \cdot & \cdot & \cdot & & \\ & & & & & & & 1 & \eta_j\Delta x & \\ & & & & -2r\eta_j\Delta x & 0 & 2r\eta_j\Delta x & 1 & & \end{bmatrix} \begin{bmatrix} u^1_j \\ v^1_j \\ u^2_j \\ v^2_j \\ \cdot \\ \cdot \\ \cdot \\ \cdot \\ u^n_j \\ v^n_j \end{bmatrix} + \begin{bmatrix} 0 \\ -r\eta_j\Delta x u^0_j \\ 0 \\ 0 \\ 0 \\ 0 \\ 0 \\ 0 \\ 0 \\ 0 \end{bmatrix}. \quad (22)$$

The eigenvalues of the above transformation matrix are calculated by numerical method. When the maximum absolute value of these eigenvalues exceeds one, the scheme is said to be unstable. We find that the range of r for stability is

$$0 < r \leq 1. \quad (23)$$

In Fig. 3, r is plotted with respect to Δx with ν = 10 W/mK, of which we can see that the admissible range of r is smaller than 1.

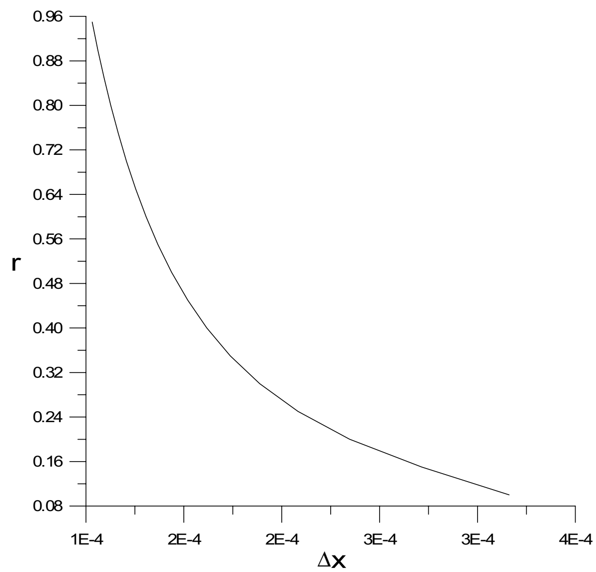

Figure 3 : The sufficient condition of stability for the group preserving scheme is $r < 11$, which is plotted with the grid spacing length vs. the stable index r.

5 Numerical examples

5.1 Example one

Let us first consider the one-dimensional heat flow equation

$$u_t = \nu u_{xx},\ 0 < x < 1, 0 < t < 1, \quad (24)$$

with the boundary conditions

$$u(0,t) = 0,\ u(1,t) = 1,$$

and the initial condition

$$u(x,0) = sin\pi x + x.$$

The exact solution is given by

$$u(x,t) = e^{-\pi^2\nu t} sin\pi x + x. \quad (25)$$

From Eq. (25) the boundary data for u^i_0 and v^i_0 can be obtained as

$$u^i_0 = u(a,\ i\Delta t) = \mathrm{e}^{-\pi^2\nu(i\Delta t)} sin\pi a + a,$$

$v_0^i = v(a,\ i\Delta t) = \pi e^{-\pi^2 \nu(i\Delta t)} cos\pi a + 1.$

In order to assess the accuracy of our numerical method, let us consider the following point-wise numerical error:

$$Error := \left| u(j\Delta x, i\Delta t) - u_j^i \right|,$$
$$j = 0,1,\ldots,N, \quad i = 1,\ldots,n, \tag{26}$$

of which u_j^i is a numerical solution at the i-th time step and at the j-th grid point; $u(j\Delta x, i\Delta t)$ is a corresponding exact solution and $||$ denotes the absolute value.

We apply the computational schemes to this example by letting $\Delta x = 10^{-3}m, \Delta t = 0.02$ sec, and a = 0.2, 0.5, 0.9 m. The numerical errors being the differences of numerical solutions and exact solutions are plotted in Fig. 4 for GPS, Euler and RK4 with two different thermal conductivities of ν = 1, 1.5 W/mK. The errors for GPS are slightly smaller than that of Euler and RK4 in a partial range.

Furthermore, we make a comparison of the numerical errors of GPS, Euler and RK4 schemes in Tables 1 and 2 for three values of $a = 0.2, 0.5, 0.9m$ with ν = 1, 1.5 W/mK and for different grid spacing lengths and time step sizes. The errors are defined by the absolute values of the differences of numerical solutions to the exact solution $u(1,t) = 1$ at $x = 1$ and $t = 0.3$ sec. From Table 1, it can be seen that the errors of GPS are less than those of the Euler and RK4 schemes for all cases. As can been seen, the errors of the Euler scheme are reduced when the time step sizes decrease or when the grid spacing lengths decrease. However, the errors of GPS are reduced when the grid spacing length increase and time step sizes decrease. But these are not true for RK4.

Next, we compare the numerical errors of GPS and RK4 schemes in Tables 3 and 4 with $\Delta x = 10^{-3}$ m, $\Delta t = 0.02sec, a = 0.2, 0.5m$ and ν = 1, 1.5 W/mK at three different times of $t = 0.1, 0.2, 0.3sec$ for three different grid points of $x = 0.6, 0.8, 1$. When $a = 0.9m$, we compare the errors at three different grid points of $x = 0.91, 0.95, 1$. It can be seen that for most of the data, GPS is more accurate than RK4. Only in the case of $a = 0.9m$ at three different grid points of $x = 0.91, 0.95, 1$, these three schemes are almost given results equal to the exact solutions.

Then, let us consider the following global error:

$$Error := \sum_{i=1}^{n} \sum_{j=1}^{N} [u_j^i - u(j\Delta x, i\Delta t)]^2. \tag{27}$$

In Tables 5 and 6, we compare the global errors of GPS, Euler and RK4 with $\Delta t = 0.02sec, a = 0.2, 0.5, 0.9m$ and ν = 1, 1.5 W/mK. The errors of GPS are smaller than those of RK4 when $a = 0.2, 0.5m$.

In a practical use, we usually mount a thermocouple as far away from the surface as possible for not destroying the structure of the engineering appliance too much, which means that a is much smaller than 1. In this sense the point-wise and global errors of GPS are much smaller than that of Euler and RK4 schemes, which in turns greatly suggest us to use the GPS in these calculations of sideways heat equation when a is limited to be small for a safety reason.

In the cases of the input data contaminated by random noises, we are concerned with the robustness of our numerical schemes. We use the function RANDOM_NUMBER given in Fortran to generate the noisy data R(i), in which R(i) are random numbers in [0, 1]. The numerical errors of GPS with random noise effect in the range of [0, 0.01] obtained from R(i) by multiplying a factor 10^{-2}, those of GPS with random noise effect on the initial condition, and those without random noise effect are plotted in Figs. 5(a)-(b), (e)-(f), and (i)-(j), respectively, for GPS at $x = 1, a = 0.2, 0.5, 0.9m$ and ν = 1, 1.5 W/mK. As can be seen, the random noise affects the numerical results very little. The numerical errors of GPS with random noise effect in the range of [0, 0.01], those on the initial condition, and those without random noise effect are plotted in Figs. 5(c)-(d), (g)-(h), and (k)-(l), respectively, for GPS at $t = 0.04sec, a = 0.2, 0.5, 0.9m$ and ν = 1, 1.5 W/mK. As shown in these figures, the random noise affects the numerical results obviously only at the rear portion of the rod when a = 0.2 and 0.5 m. For $a =$ 0.9 m, the random noise gives no influence on the numerical results. Then we imposed the random noise in the range of [0, 0.001] on the boundary data at $a = 0.2$, 0.5, 0.9 m with ν = 1, 1.5 W/mK. The numerical errors of GPS with random noise effect in the range of [0, 0.001], those with random noise effect on the boundary data and those without random noise effect are plotted in Fig. 6. Even under the disturbance of random noise, our scheme is still performing very well.

5.2 Example two

Let us consider another one-dimensional heat flow equation

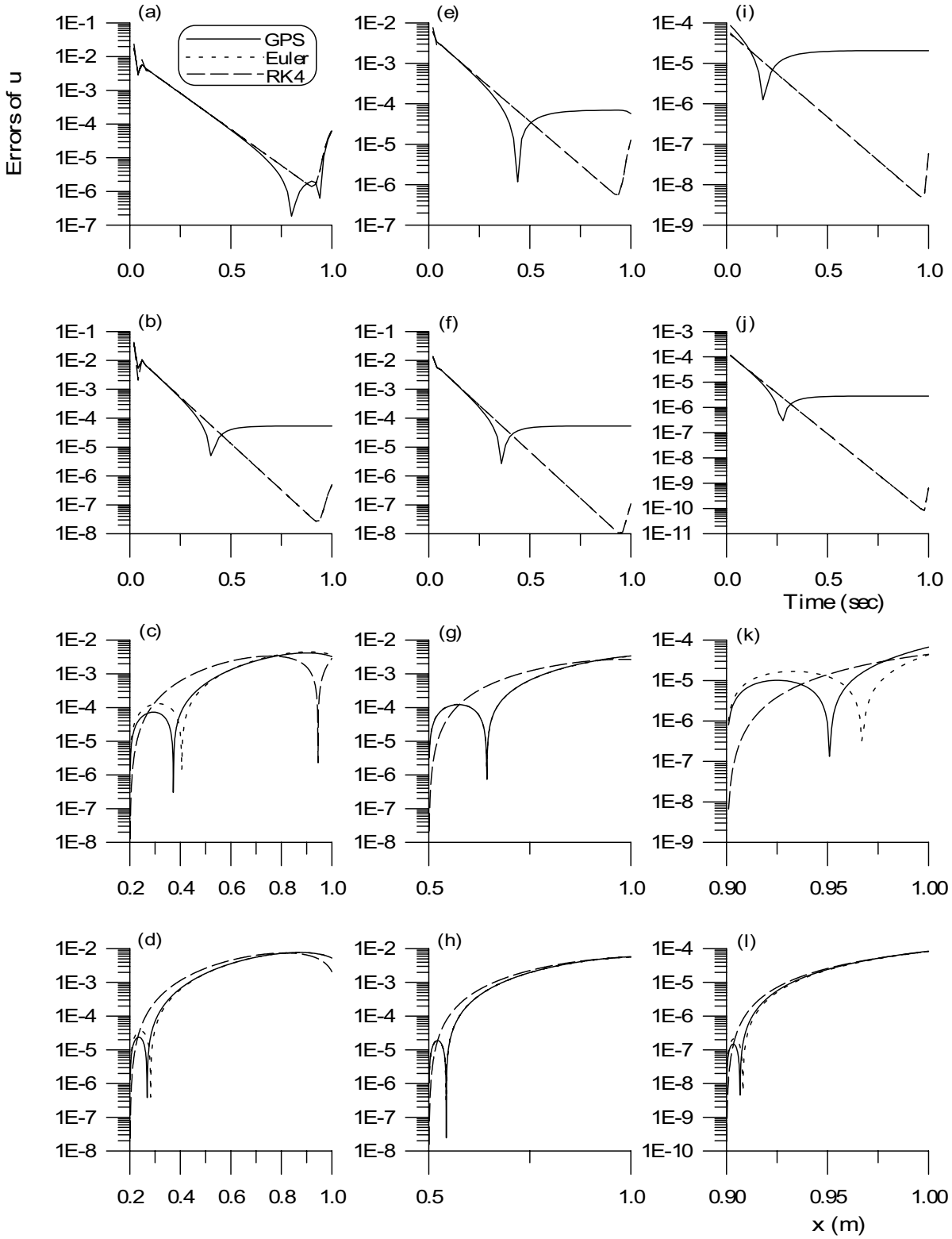

Figure 4 : Numerical errors for Example one are plotted in (a)-(b), (e)-(f), and (i)-(j) for cases of ν = 1, 1.5 W/mK with a = 0.2, 0.5, and 0.9 m, and (c)-(d), (g)-(h), (k)-(l) for cases of ν = 1, 1.5 W/mK with $a = 0.2, 0.5, 0.9m$.

Table 1: Comparing the numerical errors of GPS, Euler and RK4 schemes for v = 1 W/mK with a = 0.2, 0.5 and 0.9 m of Example one.

Δt	Δx	Error of GPS	Error of Euler	Error of RK4	
0.025	0.8/600	7.78873E-4	7.86012E-4	7.82614E-4	
	0.8/700	7.79535E-4	7.85621E-4	7.82614E-4	
	0.8/800	7.80003E-4	7.85307E-4	7.82614E-4	
	0.8/900	7.80351E-4	7.85050E-4	7.82614E-4	
	0.8/1000	7.80619E-4	7.84837E-4	7.82614E-4	
0.02	0.8/600	4.99399E-4	5.03331E-4	5.01438E-4	*a=0.2*
	0.8/700	4.99834E-4	5.03154E-4	5.01438E-4	
	0.8/800	5.00128E-4	5.03001E-4	5.01438E-4	
	0.8/900	5.00338E-4	5.02870E-4	5.01438E-4	
	0.8/1000	5.00494E-4	5.02758E-4	5.01438E-4	
0.025	0.5/600	3.64367E-4	4.13470E-4	4.12800E-4	
	0.5/700	3.71312E-4	4.13397E-4	4.12800E-4	
	0.5/800	3.76516E-4	4.13338E-4	4.12800E-4	
	0.5/900	3.80560E-4	4.13289E-4	4.12800E-4	
	0.5/1000	3.83792E-4	4.13247E-4	4.12800E-4	*a=0.5*
0.02	0.5/600	2.15360E-4	2.64505E-4	2.64145E-4	
	0.5/700	2.22358E-4	2.64476E-4	2.64145E-4	
	0.5/800	2.27599E-4	2.64450E-4	2.64145E-4	
	0.5/900	2.31673E-4	2.64427E-4	2.64145E-4	
	0.5/1000	2.34929E-4	2.64406E-4	2.64145E-4	
0.025	0.1/600	2.42706E-6	5.33799E-6	5.33905E-6	
	0.1/700	2.84330E-6	5.33832E-6	5.33905E-6	
	0.1/800	3.15543E-6	5.33854E-6	5.33905E-6	
	0.1/900	3.39817E-6	5.33868E-6	5.33905E-6	
	0.1/1000	3.59233E-6	5.33877E-6	5.33905E-6	*a=0.9*
0.02	0.1/600	5.16323E-7	3.41216E-6	3.41337E-6	
	0.1/700	9.30435E-7	3.41252E-6	3.41337E-6	
	0.1/800	1.24096E-6	3.41274E-6	3.41337E-6	
	0.1/900	1.48246E-6	3.41290E-6	3.41337E-6	
	0.1/1000	1.67563E-6	3.41300E-6	3.41337E-6	

Table 2: Comparing the numerical errors of GPS, Euler and RK4 schemes for v = 1.5 W/mK with a = 0.2, 0.5 and 0.9 m of Example one.

Δt	Δx	Error of GPS	Error of Euler	Error of RK4	
0.025	0.8/600	3.27287E-4	4.01058E-4	3.99082E-4	
	0.8/700	3.37576E-4	4.00797E-4	3.99082E-4	
	0.8/800	3.45286E-4	4.00596E-4	3.99082E-4	
	0.8/900	3.51278E-4	4.00437E-4	3.99082E-4	
	0.8/1000	3.56069E-4	4.00309E-4	3.99082E-4	*a=0.2*
0.02	0.8/600	1.88111E-4	2.57266E-4	2.56071E-4	
	0.8/700	1.97861E-4	2.57116E-4	2.56071E-4	
	0.8/800	2.05164E-4	2.57000E-4	2.56071E-4	
	0.8/900	2.10839E-4	2.56906E-4	2.56071E-4	
	0.8/1000	2.15376E-4	2.56830E-4	2.56071E-4	
0.025	0.5/600	1.42660E-4	2.11865E-4	2.11463E-4	
	0.5/700	1.52498E-4	2.11813E-4	2.11463E-4	
	0.5/800	1.59875E-4	2.11773E-4	2.11463E-4	
	0.5/900	1.65611E-4	2.11741E-4	2.11463E-4	
	0.5/1000	1.70199E-4	2.11715E-4	2.11463E-4	*a=0.5*
0.02	0.5/600	6.63999E-5	1.35524E-4	1.35285E-4	
	0.5/700	7.62505E-5	1.35495E-4	1.35285E-4	
	0.5/800	8.36363E-5	1.35472E-4	1.35285E-4	
	0.5/900	8.93795E-5	1.35454E-4	1.35285E-4	
	0.5/1000	9.39732E-5	1.35438E-4	1.35285E-4	
0.025	0.1/600	8.64911E-7	2.74333E-6	2.74345E-6	
	0.1/700	3.49336E-7	2.74339E-6	2.74345E-6	
	0.1/800	3.73248E-8	2.74342E-6	2.74345E-6	
	0.1/900	3.38048E-7	2.74345E-6	2.74345E-6	
	0.1/1000	5.78619E-7	2.74346E-6	2.74345E-6	*a=0.9*
0.02	0.1/600	1.83971E-6	1.75143E-6	1.75163E-6	
	0.1/700	1.32656E-6	1.75150E-6	1.75163E-6	
	0.1/800	9.41719E-7	1.75154E-6	1.75163E-6	
	0.1/900	6.42413E-7	1.75157E-6	1.75163E-6	
	0.1/1000	4.02976E-7	1.75159E-6	1.75163E-6	

Table 3: Comparing the computational results of GPS and RK4 schemes with the exact solution for v = 1 W/mK with a = 0.2, 0.5 and 0.9 m of Example one.

t	x	GPS	RK4	Exact	
0.1	0.6	0.95372	0.95306	0.95447	
	0.8	1.10169	1.10163	1.10191	
	1	0.99639	0.99633	1.00000	
0.2	0.6	0.73179	0.73159	0.73211	
	0.8	0.88083	0.88062	0.88165	a=0.2
	1	0.99865	0.99865	1.00000	
0.3	0.6	0.64908	0.64904	0.64924	
	0.8	0.83010	0.83005	0.83043	
	1	0.99950	0.99950	1.00000	
0.1	0.6	0.95446	0.95435	0.95447	
	0.8	1.10184	1.10182	1.10191	
	1	0.99809	0.99810	1.00000	
0.2	0.6	0.73211	0.73207	0.73211	
	0.8	0.88139	0.88131	0.88165	a=0.5
	1	0.99932	0.99929	1.00000	
0.3	0.6	0.64924	0.64922	0.64924	
	0.8	0.83035	0.83030	0.83043	
	1	0.99977	0.99974	1.00000	
0.1	0.91	0.10140	0.10140	0.10140	
	0.95	0.10083	0.10083	0.10083	
	1	0.99998	0.99998	1.00000	
0.2	0.91	0.94876	0.94876	0.94876	
	0.95	0.97173	0.97173	0.97173	a=0.9
	1	0.99999	0.99999	1.00000	
0.3	0.91	0.92444	0.92444	0.92444	
	0.95	0.95810	0.95810	0.95810	
	1	1.00000	0.99999	1.00000	

Table 4: Comparing the computational results of GPS and RK4 schemes with the exact solution for v = 1.5 W/mK with a = 0.2, 0.5 and 0.9 m of Example one.

t	x	GPS	RK4	Exact	
0.1	0.6	0.81488	0.81447	0.81640	
	0.8	0.93032	0.92993	0.93374	
	1	0.99504	0.99504	1.00000	
0.2	0.6	0.64887	0.64880	0.64924	
	0.8	0.82966	0.82956	0.83043	*a=0.2*
	1	0.99892	0.99888	1.00000	
0.3	0.6	0.61110	0.61110	0.61120	
	0.8	0.80676	0.80673	0.80692	
	1	0.99980	0.99974	1.00000	
0.1	0.6	0.81631	0.81624	0.81640	
	0.8	0.93261	0.93247	0.93374	
	1	0.99740	0.99739	1.00000	
0.2	0.6	0.64922	0.64920	0.64924	
	0.8	0.83019	0.83014	0.83043	*a=0.5*
	1	0.99945	0.99941	1.00000	
0.3	0.6	0.61120	0.61119	0.61120	
	0.8	0.80689	0.80686	0.80692	
	1	0.99992	0.99987	1.00000	
0.1	0.91	0.97348	0.97348	0.97348	
	0.95	0.98559	0.98558	0.98560	
	1	0.99997	0.99997	1.00000	
0.2	0.91	0.92444	0.92444	0.92444	
	0.95	0.95810	0.95810	0.95810	*a=0.9*
	1	1.00000	0.99999	1.00000	
0.3	0.91	0.91329	0.91329	0.91329	
	0.95	0.95184	0.95184	0.95184	
	1	1.00000	0.99999	1.00000	

Table 5: Comparing the global errors of GPS, Euler and RK4 schemes for v = 1 W/mK with a = 0.2, 0.5 and 0.9 m of Example one.

Δx	Error of GPS	Error of Euler	Error of RK4	
0.8/600	0.03196	0.03178	0.08047	
0.8/700	0.04262	0.04222	0.09383	
0.8/800	0.05396	0.05339	0.10718	*a=0.2*
0.8/900	0.06575	0.06505	0.12054	
0.8/1000	0.07785	0.07704	0.13389	
0.5/600	0.008262	0.008055	0.012122	
0.5/700	0.010179	0.009968	0.014135	
0.5/800	0.012120	0.011906	0.016148	*a=0.5*
0.5/900	0.014077	0.013861	0.018161	
0.5/1000	0.016045	0.015827	0.020174	
0.1/600	1.304E-6	1.069E-6	1.298E-6	
0.1/700	1.503E-6	1.280E-6	1.514E-6	
0.1/800	1.707E-6	1.493E-6	1.730E-6	*a=0.9*
0.1/900	1.913E-6	1.706E-6	1.945E-6	
0.1/1000	2.121E-6	1.920E-6	2.161E-6	

$$u_t = \nu u_{xx},\ 0 < x < 2,\ 0 < t < 1, \tag{28}$$

with the boundary conditions

$$u(0,t) = u(2,t) = 0,$$

and the initial condition

$$u(x,0) = \begin{cases} 100x, for 0 \le x \le 1, \\ 100(2-x), for 1 \le x \le 2. \end{cases}$$

The exact solution is given by

$$\begin{aligned} u(x,t) &= 800 \sum_{p=0}^{\infty} \frac{1}{\pi^2(2p+1)^2} \cos \frac{(2p+1)\pi(x-1)}{2} \\ &\quad \times \exp[-\pi^2 \nu (2p+1)^2 t/4], \\ v(x,t) &= -800 \sum_{p=0}^{\infty} \frac{1}{2\pi(2p+1)} \sin \frac{(2p+1)\pi(x-1)}{2} \\ &\quad \times \exp[-\pi^2 \nu (2p+1)^2 t/4]. \end{aligned} \tag{29}$$

From Eq. (28) the boundary data for u_0^i and v_0^i can be obtained

Table 6: Comparing the global errors of GPS, Euler and RK4 schemes for ν = 1.5 W/mK with a = 0.2, 0.5 and 0.9 m of Example one.

Δx	Error of GPS	Error of Euler	Error of RK4	
0.8/600	0.16204	0.16042	0.23866	
0.8/700	0.20026	0.19855	0.27828	
0.8/800	0.23882	0.23706	0.31789	*a=0.2*
0.8/900	0.27762	0.27581	0.35750	
0.8/1000	0.31658	0.31474	0.39711	
0.5/600	0.03111	0.03074	0.03673	
0.5/700	0.03716	0.03678	0.04283	
0.5/800	0.04322	0.04284	0.04893	*a=0.5*
0.5/900	0.04928	0.04891	0.05503	
0.5/1000	0.05536	0.05498	0.06113	
0.1/600	3.926E-6	3.623E-6	3.957E-6	
0.1/700	4.564E-6	4.278E-6	4.614E-6	
0.1/800	5.207E-6	4.933E-6	5.271E-6	*a=0.9*
0.1/900	5.854E-6	5.589E-6	5.929E-6	
0.1/1000	6.502E-6	6.246E-6	6.586E-6	

$$u_0^i = u(a,\, i\Delta t) = 800 \sum_{p=0}^{\infty} \frac{1}{\pi^2(2p+1)^2} \cos\frac{(2p+1)\pi(a-1)}{2} \times \exp[-\pi^2 \nu (2p+1)^2 (i\Delta t)/4],$$

$$v_0^i = v(a,\, i\Delta t) = -800 \sum_{p=0}^{\infty} \frac{1}{2\pi(2p+1)} \sin\frac{(2p+1)\pi(a-1)}{2} \times \exp[-\pi^2 \nu (2p+1)^2 (i\Delta t)/4].$$

We apply the computational schemes to this example by letting $\Delta x = 10^{-3} m, \Delta t = 0.02$ sec, and a = 1.4, 1.6, 1.9 m. The numerical errors are plotted in Fig. 7 for GPS, Euler and RK4 with two different thermal conductivities of ν = 1, 1.5 W/mK. The errors for GPS are slightly smaller than those of Euler and RK4 in the partial range. At three different times of t = 0.1, 0.2, 0.3 sec, we compare the numerical errors of GPS and RK4 in Tables 7 and 8 for ν = 1, 1.5 W/mK, respectively, with fixed values of Δx = 10^{-3} m, Δt = 0.02 sec, a = 1.4 m at three different grid points of x = 1.5, 1.7, 2, a = 1.6 m at grid points of x = 1.7, 1.9, 2, and a = 1.9 m at grid points of x = 1.91, 1.95, 2. It can be seen that for most of the numerical data, GPS is more accurate than Euler. Only in the cases of a = 1.4, 1.6, 1.9 m at grid point of x = 2 and time of t = 0.3 sec, the errors for Euler are slightly smaller than those of GPS.

The numerical errors of GPS with random noise effect in the range of [0, 1], those on the initial condition, and those without random noise effect are plotted in Figs. 8(a)-(b), (e)-(f), and (i)-(j) for GPS, respectively, at $x = 2, a = 1.4, 1.6, 1.9m$ and ν = 1, 1.5 W/mK. It is found that the random noise does not affect the numerical results. As for the numerical errors of GPS with ran-

Table 7: Comparing the computational results of GPS and Euler schemes with the exact solution for v = 1 W/mK with a = 1.4, 1.6 and 1.9 m of Example two.

t	x	GPS	Euler	Exact	
0.1	1.5	44.0922	44.0940	44.0874	
	1.7	27.8124	27.8175	27.7920	
	2	2.7876E-2	3.5082E-2	0.0000	
0.2	1.5	34.9191	34.9204	34.9162	
	1.7	22.3654	22.3695	22.3610	a=1.4
	2	5.1014E-3	7.4147E-4	0.0000	
0.3	1.5	27.3342	27.3353	27.3321	
	1.7	17.5445	17.5476	17.5421	
	2	7.6413E-3	3.0504E-3	0.0000	
0.1	1.7	27.7964	27.7977	27.7920	
	1.9	9.4900	9.4928	9.4685	
	2	2.7795E-2	3.0788E-2	0.0000	
0.2	1.7	22.3629	22.3639	22.3610	
	1.9	7.6952	7.6975	7.6930	a=1.6
	2	1.4362E-4	2.2932E-3	0.0000	
0.3	1.7	17.5434	17.5442	17.5421	
	1.9	6.0433	6.0451	6.0433	
	2	2.6811E-3	7.6629E-4	0.0000	
0.1	1.91	8.52593	8.52596	8.52588	
	1.95	4.74377	4.74390	4.74347	
	2	6.14062E-4	7.96917E-4	0.00000	
0.2	1.91	6.92892	6.92894	6.92886	
	1.95	3.85794	3.85805	3.85779	a=1.9
	2	5.15664E-5	9.72179E-5	0.00000	
0.3	1.91	5.44324	5.44326	5.44319	
	1.95	3.03102	3.03111	3.03092	
	2	1.19365E-4	2.46244E-6	0.00000	

Table 8: Comparing the computational results of GPS and Euler schemes with the exact solution for v = 1.5 W/mK with a = 1.4, 1.6 and 1.9 m of Example two.

t	x	GPS	Euler	Exact	
0.1	1.5	39.3615	39.3632	39.3578	
	1.7	25.1115	25.1162	25.0977	
	2	1.6261E-2	2.3208E-2	0.0000	
0.2	1.5	27.3340	27.3351	27.3321	
	1.7	17.5431	17.5464	17.5421	*a=1.4*
	2	1.1800E-2	6.9245E-3	0.0000	
0.3	1.5	18.8838	18.8845	18.8824	
	1.7	12.1234	12.1257	12.1231	
	2	9.0019E-3	5.6319E-3	0.0000	
0.1	1.7	25.1016	25.1027	25.0977	
	1.9	8.6279	8.6305	8.6116	
	2	1.9017E-2	2.1867E-2	0.0000	
0.2	1.7	17.5433	17.5441	17.5421	
	1.9	6.0426	6.0445	6.0433	*a=1.6*
	2	3.7546E-3	1.7519E-3	0.0000	
0.3	1.7	12.1238	12.1244	12.1231	
	1.9	4.1764	4.1777	4.1773	
	2	3.2018E-3	1.8174E-3	0.0000	
0.1	1.91	7.75576	7.75579	7.75570	
	1.95	4.31761	4.31774	4.31729	
	2	5.49258E-4	7.23620E-4	0.00000	
0.2	1.91	5.44323	5.44326	5.44319	
	1.95	3.03102	3.03111	3.03092	*a=1.9*
	2	1.33856E-4	1.14123E-5	0.00000	
0.3	1.91	3.76252	3.76253	3.76249	
	1.95	2.09515	2.09521	2.09509	
	2	1.11512E-4	2.68724E-5	0.00000	

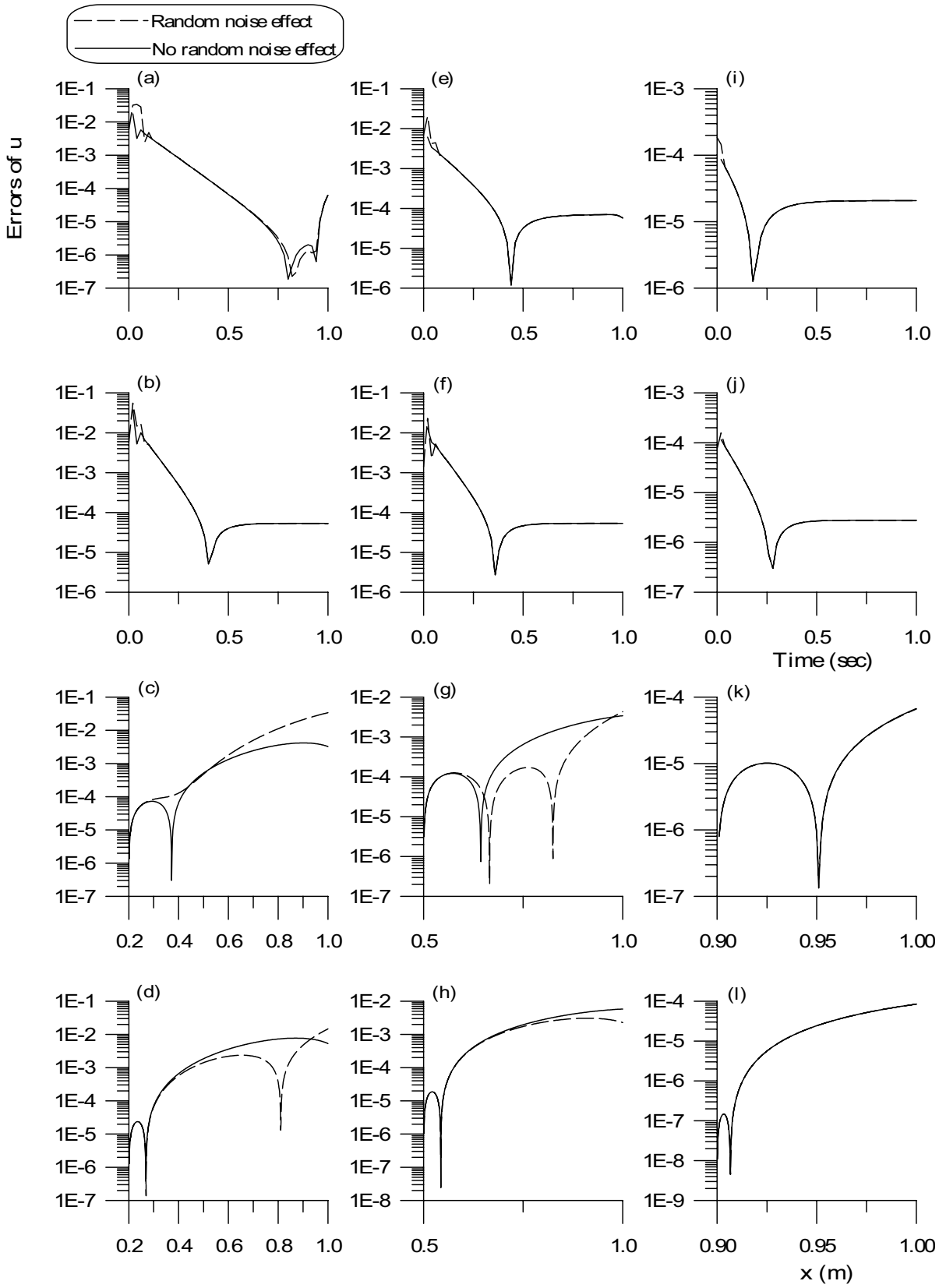

Figure 5 : Errors of GPS solutions with and without random noise effect for Example one are plotted in (a)-(b), (e)-(f), and (i)-(j) for cases of ν = 1, 1.5 W/mK with a = 0.2, 0.5, and 0.9 m, and (c)-(d), (g)-(h), (k)-(l) for cases of ν = 1, 1.5 W/mK with a = 0.2, 0.5, and 0.9 m.

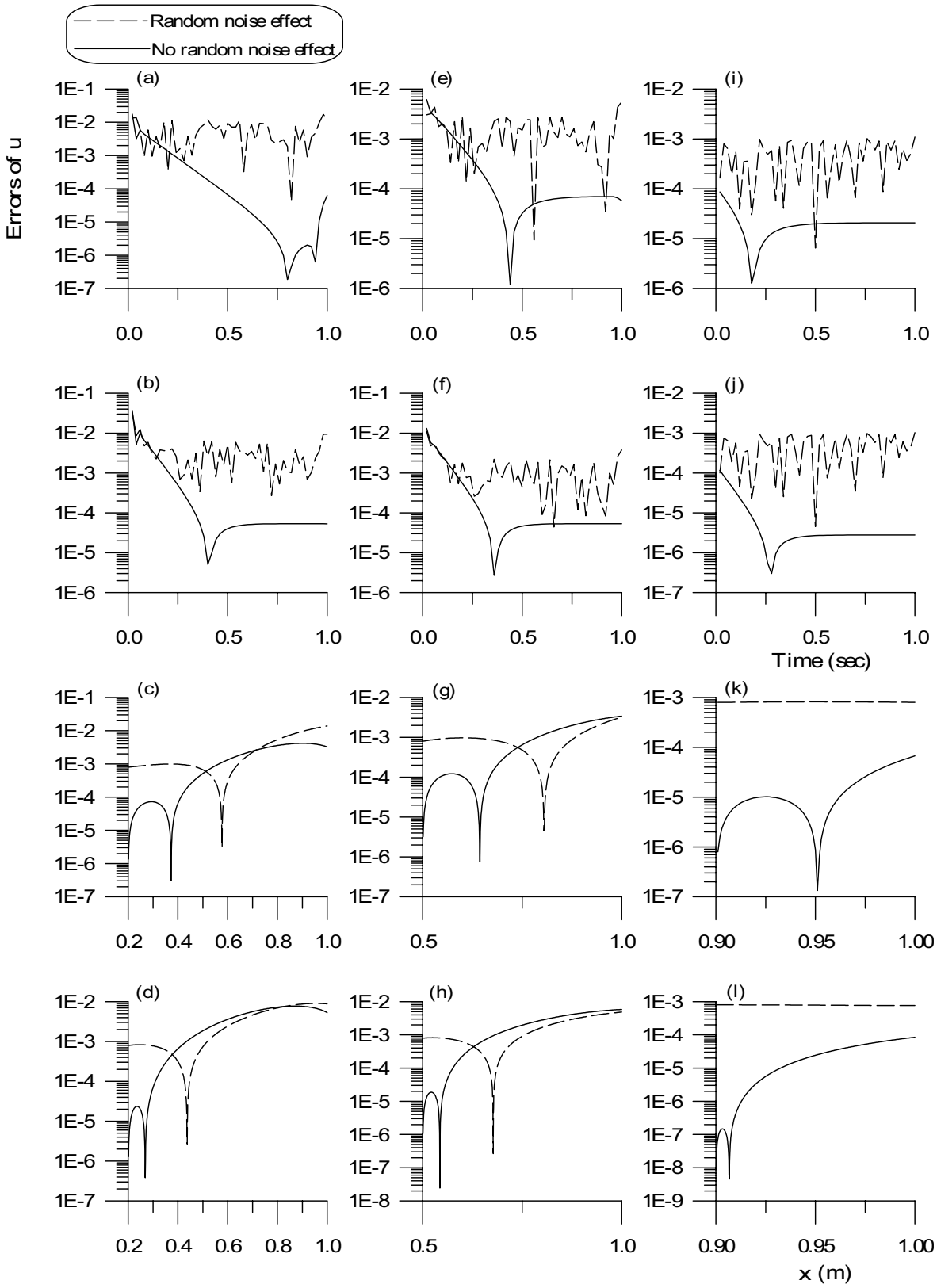

Figure 6 : Errors of GPS solutions with and without random noise effect on the boundary data for Example one are plotted in (a)-(b), (e)-(f), and (i)-(j) for cases of ν = 1, 1.5 W/mK with a = 0.2, 0.5, and 0.9 m, and (c)-(d), (g)-(h), (k)-(l) for cases of ν = 1, 1.5 W/mK with a = 0.2, 0.5, and 0.9 m.

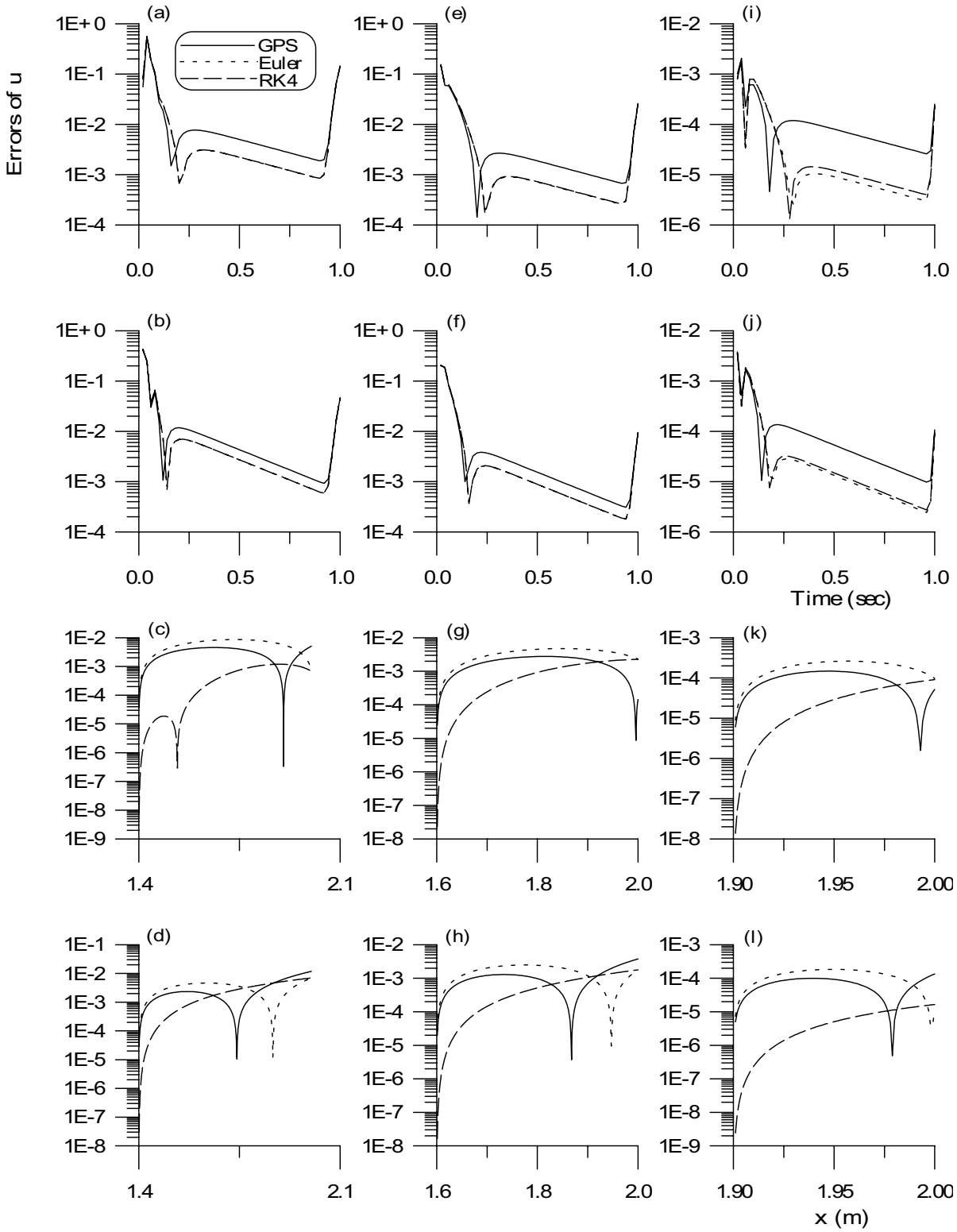

Figure 7 : Numerical errors for Example two are plotted in (a)-(b), (e)-(f), and (i)-(j) for cases of ν = 1, 1.5 W/mK with *a* = 1.4, 1.6, and 1.9 m, and (c)-(d), (g)-(h), (k)-(l) for cases of ν = 1, 1.5 W/mK with *a* = 1.4, 1.6, and 1.9 m.

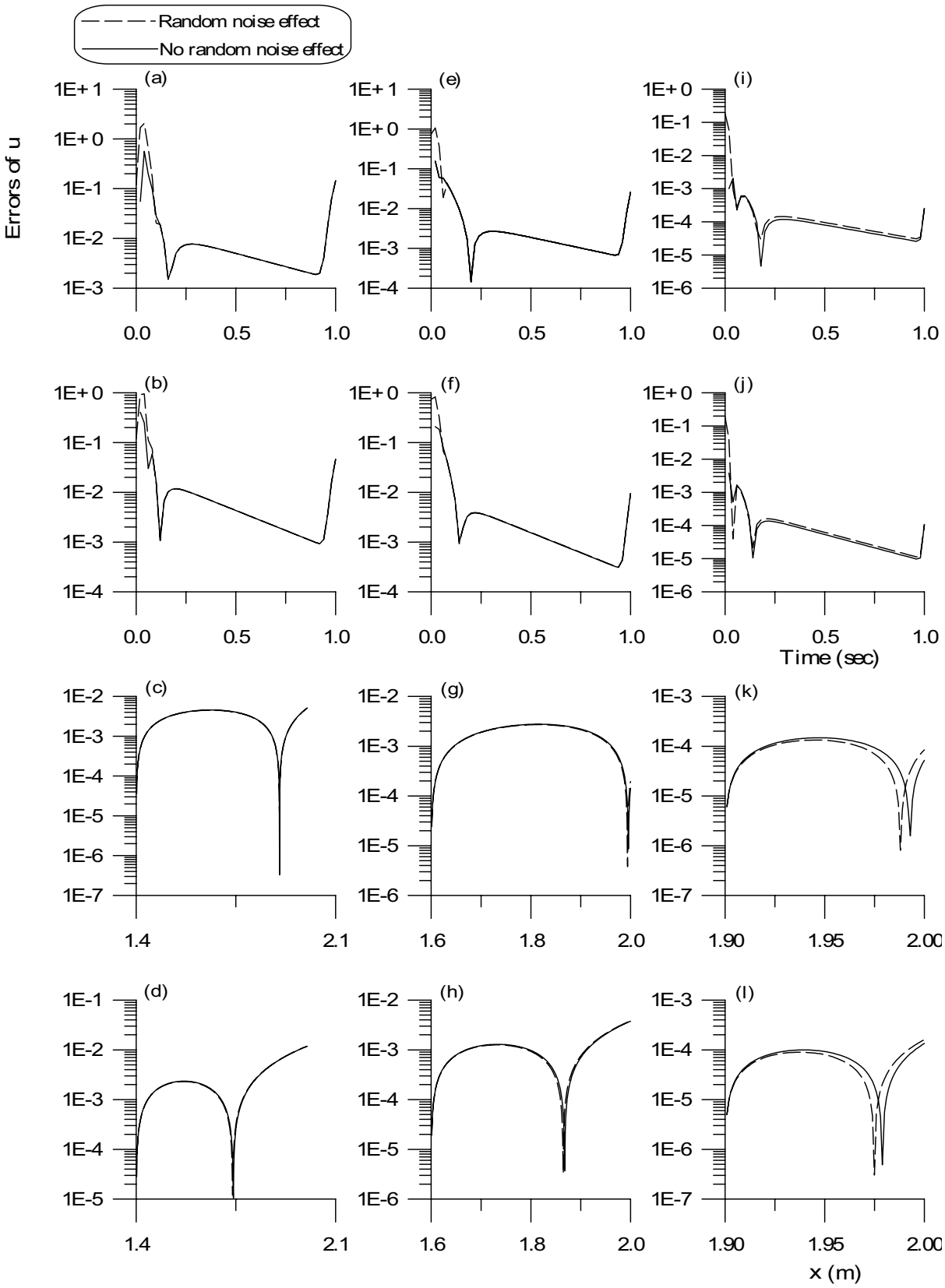

Figure 8 : Errors of GPS solutions with and without random noise effect for Example two are plotted in (a)-(b), (e)-(f), and (i)-(j) for cases of ν = 1, 1.5 W/mK with a = 1.4, 1.6, and 1.9 m, and (c)-(d), (g)-(h), (k)-(l) for cases of ν = 1, 1.5 W/mK with a = 1.4, 1.6, and 1.9 m.

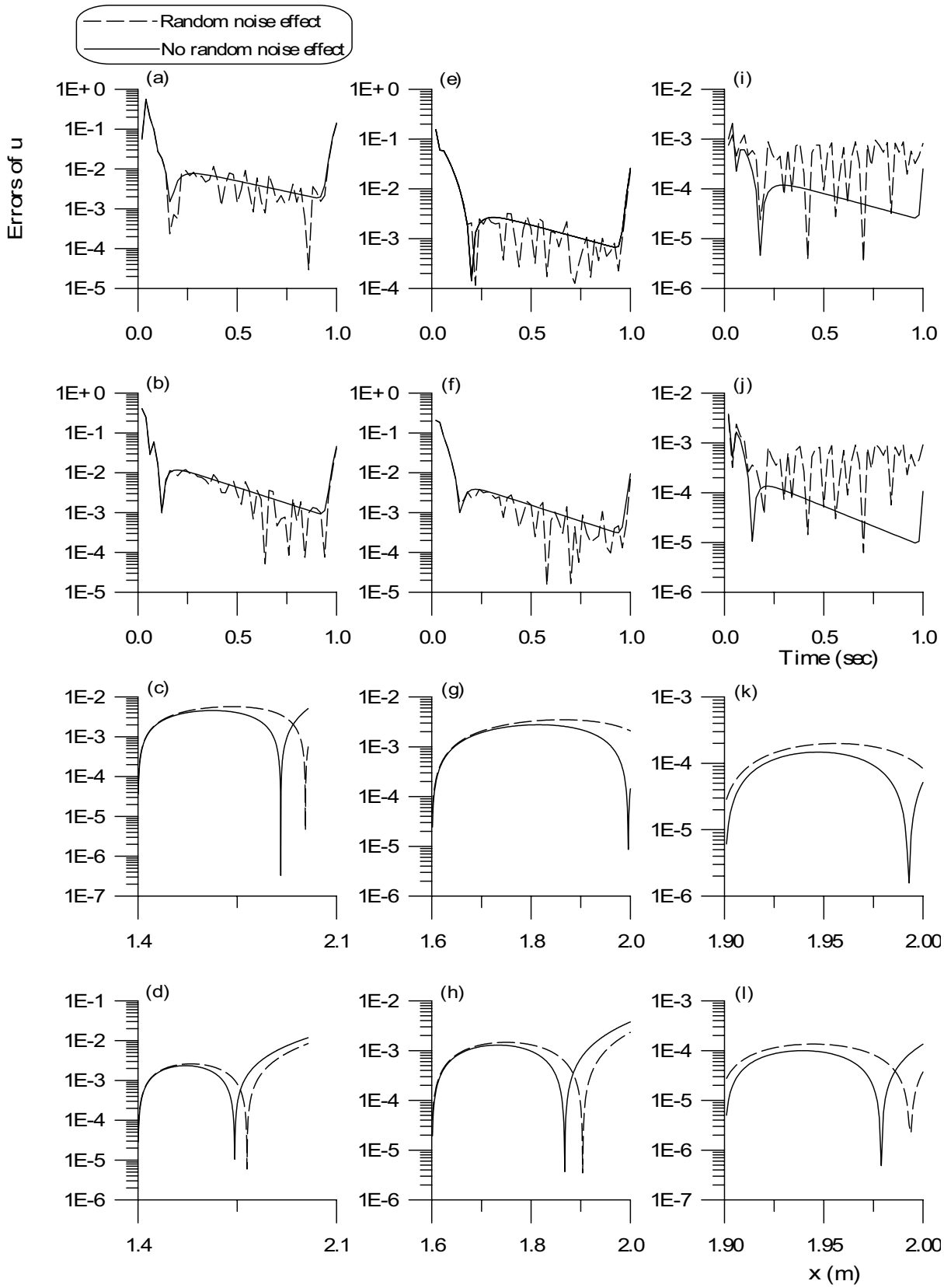

Figure 9 : Errors of GPS solutions with and without random noise effect on the boundary data for Example two are plotted in (a)-(b), (e)-(f), and (i)-(j) for cases of ν = 1, 1.5 W/mK with a = 1.4, 1.6, and 1.9 m, and (c)-(d), (g)-(h), (k)-(l) for cases of ν = 1, 1.5 W/mK with a = 1.4, 1.6, and 1.9 m.

dom noise effect and those without random noise effect, all are plotted in Figs. 8(c)-(d), (g)-(h), (k)-(l) for GPS, respectively, at $t = 0.2sec, a = 1.4, 1.6, 1.9m$ and ν = 1, 1.5 W/mK. As shown, the random noise affects the numerical results slightly. When we impose the random noise in the range of [0, 0.001] on the boundary data at $a = 1.4, 1.6, 1.9m$ with ν = 1, 1.5 W/mK, the numerical errors of GPS with random noise effect in the range of [0, 0.001], those on the boundary data, and those without random noise effect are plotted in Fig. 9. It can be seen that the disturbance from the noise may influence the numerical results, but the scheme is robust.

6 Conclusions

The inverse heat conduction problems have been well calculated by the formulation with a semi-discretization of the time coordinate of sideways heat equation in conjunction with the group preserving numerical integration scheme along the spatial direction. In the inverse numerical integration of the sideways heat equation, a simple employment of the finite difference, finite element, boundary element or meshless method may result in numerical instablility. Embedding the time discretized heat conduction equation into an augmented system in the Minkowski space, we can develop spatial-stepping numerical integration under the Lie group theory and admit a large spatial stepsize without inducing instability, which is guaranteed by the group properties. Numerical results indicate that the group preserving scheme is efficient to numerically integrating the sideways heat equation and is also better than RK4. The numerical behavior of GPS is very unlike that of the conventional numerical methods, *e*.g., RK4 and the Euler scheme. It is found that the numerical errors of GPS are reduced when the grid spacing lengths are increased. Besides, under a reasonable time stepsize and grid spacing length, the GPS can produce a good result. The implementation is quite easy and is also robust to defend the noise disturbance. The efficiency of GPS is rooted in the closure property of the Lie group that we used it to construct the numerical method for IHCP. Therefore, it is highly advocated to be used in the numerical computations of sideways heat equation. Especially, when the thermocouple is mounted in a position far away from the surface for a safety reason, the GPS provided computational results much better than others.

References

Al-Khalidy, N. (1998a): A general space marching algorithm for the solution of two-dimensional boundary inverse heat conduction problems. *Numerical Heat Transfer*, *Part B*, vol. 34, pp. 339-360.

Al-Khalidy, N. (1998b): On the solution of parabolic and hyperbolic inverse heat conduction problems. *International Journal of Heat and Mass Transfer*, vol. 41, pp. 3731-3740.

AL-Najem, N. M.; Osman, A. M.; El-Refaee, M. M.; Khanafer, K. M. (1998): Two dimensional steady-state inverse heat conduction problems. *International Communications in Heat and Mass Transfer*, vol. 25, pp. 541-550.

Battaglia, J. L.; Cois, O.; Puigsegur, L.; Oustaloup, A. (2001): Solving an inverse heat conduction problem using a non-integer identified model. *International Journal of Heat and Mass Transfer*, vol. 44, pp. 2671-2680.

Battaglia, J. L. (2002): A modal approach to solve inverse heat conduction problems. *Inverse Problems in Engineering*, vol. 10, pp. 41-63.

Beck, J. V.; Blackwell, B.; Clair, C. R. St. (1985): *Inverse Heat Conduction: Ill-Posed Problem*. Wiley, New York.

Behbahani-nia, A.; Kowsary, F. (2004): A dual reciprocity BE-based sequential function specification solution method for inverse heat conduction problems. *International Journal of Heat and Mass Transfer*, vol. 47, pp. 1247-1255.

Berntsson, F. (1999): A spectral method for solving the sideways heat equation. *Inverse Problems*, vol. 15, pp. 891-906.

Berntsson, F. (2003): Sequential solution of the sideways heat equation by windowing of the data. *Inverse Problems in Engineering*, vol. 11, pp. 91-103.

Blanc, G.; Raynaud, M.; Chau, T.H. (1998): A guide for the use of the function specification method for 2D inverse heat conduction problems. *Revue Générale de Thermique*, vol. 37, pp. 17-30.

Brebbia, C. A. (1984): Applications of the boundary element method for heat transfer problems. *Proceedings of the Conference Modelisation et Simulation en Thermique*, Ensma, Poitiers, pp. 1-18.

Cannon, J. R. (1963): The solution of the heat equation subject to the specification of energy. *Quarterly Applied*

Mathematics, vol. 21, pp. 155-160.

Carasso, A. S. (1992): Space marching difference schemes in the nonlinear inverse heat conduction problem. *Inverse Problems*, vol. 8, pp. 25-43.

Carasso, A. S. (1993): Slowly divergent space marching schemes in the inverse heat conduction problem. *Numerical Heat Transfer*, *Part B*, vol. 23, pp. 111-126.

Chantasiriwan, S. (1999): Inverse heat conduction problem of determining time-dependent heat transfer coefficient. *International Journal of Heat and Mass Transfer*, vol. 42, pp. 4275-4285.

Chantasiriwan, S. (2001): An algorithm for solving multidimensional inverse heat conduction problem. *International Journal of Heat and Mass Transfer*, vol. 44, pp. 3823-3832.

Chen, H.-T.; Lin, S.-Y.; Fang, L.-C. (2001): Estimation of surface temperature in two-dimensional inverse heat conduction problems. *International Journal of Heat and Mass Transfer*, vol. 44, pp. 1455-1463.

Chen, H.-T.; Peng, S.-Y.; Yang, P.-C.; Fang, L.-C. (2001): Numerical method for hyperbolic inverse heat conduction problems. *International Communications in Heat and Mass Transfer*, vol. 28, pp. 847-856.

Chen, H.-T.; Lin, S.-Y. Wang, H.-R.; Fang, L.-C. (2002): Estimation of two-sided boundary conditions for two-dimensional inverse heat conduction problems. *International Journal of Heat and Mass Transfer*, vol. 45, pp. 15-23.

Dorai, G.A.; Tortorelli, D.A. (1997): Transient inverse heat conduction problem solutions via Newton's method. *International Journal of Heat and Mass Transfer*, vol. 40, pp. 4115-4127.

Dorroh, J.R.; Ru, X. (1999): The application of the method of quasi-reversibility to the sideways heat equation. *Journal of Mathematical Analysis and Applications*, vol. 236, pp. 503-519.

Eldén, L. (1995a): Numerical solution of the sideways heat equation by difference approximation in time. *Inverse Problems*, vol. 11, pp. 913-923.

Eldén L. (1995b): Numerical solution of the sideways heat equation. *In Inverse Problems in Diffusion Processes*. *Proceedings in Applied Mathematics*, ed. H.Engl and W. Rundell, SIAM, Philadelphia.

Eldén, L. (1997): Solving an inverse heat-conduction problem by a "method of lines". *Journal Heat Transfer Transactions*, *ASME*, vol. 119, pp. 406-412.

Eldén, L.; Berntsson, F.; Reginska, T. (2000): Wavelet and Fourier methods for solving the sideways heat equation. *SIAM Journal on Scientific Computing*, vol.21, pp. 2187-2205.

Fu, C.-L.; Qiu, C.-Y.; Zhu, Y.-B. (2002): A note on "sideways heat equation and wavelets" and constant e^*. *Computers and Mathematics with Applications*, vol. 43, pp. 1125-1134.

Fu, C.-L.; Zhu, Y.-B.; Qiu, C.-Y. (2003): Wavelet regularization for an inverse heat conduction problem. *Journal of Mathematical Analysis and Applications*, vol. 288, pp. 212-222.

Guo, L.; Murio, D. A.; Roth, C. (1990): A mollified space marching finite differences algorithm for the inverse heat conduction problem with slab symmetry. *Computers and Mathematics with Applications*, vol. 19, pp. 75-89.

Guo, L.; Murio, D. A. (1991): A mollified space-marching finite-difference algorithm for the two-dimensional inverse heat conduction problem with slab symmetry. *Inverse Problems*, vol. 7, pp. 247-259.

Hadamard, J. (1953): *Lectures on Cauchy's Problem in Linear Partial Differential Equations*. Dover Publications, New York.

Hon, Y.-C.; Wei, T. (2002): A meshless computational method for solving inverse heat conduction problem. *International Series on Advances in Boundary Elements*, vol. 13, pp. 135-144.

Hon, Y.-C.; Wei, T. (2004): A fundamental solution method for inverse heat conduction problem. *Engineering Analysis with Boundary Elements*, vol. 28, pp. 489-495.

Hon, Y.-C.; Wei, T. (2005): The method of fundamental solution for solving multidimensional inverse heat conduction problems. *CMES: Computer Modeling in Engineering & Sciences*, vol. 7, pp. 119-132.

Ingham, D. B.; Yuan, Y.; Han, H. (1991): The boundary-element method for an improperly posed problem. *Journal of Applied Mathematics*, vol. 47, pp. 61-79.

Ingham, D. B.; Yuan, Y. (1994): *The Boundary Element Method for Solving Improperly Posed Problems* (Edited by C. A. Brebbia and J. J. Connor). Computational Mechanics, Southampton, vol. 19.

Jonas, P.; Louis, A. K. (1999): Approximate inverse for

a one-dimensional inverse heat conduction problem. *Inverse Problems*, vol. 15, pp. 891-906.

Kim, S. K.; Lee, W. I. (2002): Solution of inverse heat conduction problems using maximum entropy method. *International Journal of Heat and Mass Transfer*, vol. 45, pp. 381-391.

Krutz, G. W.; Schoenhals, R. J.; Hore, P. S. (1978): Application of finite element method to the inverse heat conduction problem. *Numerical Heat Transfer*, vol. 1, pp. 489-498.

Kurpisz, K.; Nowak, A. J. (1992): BEM approach to inverse heat conduction problems. *Engineering Analysis with Boundary Elements*, vol. 10, pp. 291-297.

Kurpisz, K.; Nowak, A.J. (1995): *Inverse Thermal Problems*. Computational Mechanics Publications, Souhampton, USA.

Lahoucine, C.O. (2004): A Duhamel integral based solution for the sideways heat equation applied to the non-intrusive temperature measurement. *International Communications in Heat and Mass Transfer*, vol. 31, pp. 1037-1045.

Le Niliot, C.; Papini, C.; Pasquetti, R. (1990): Boundary element method for inverse heat conduction problems. *In Advanced Computational Methods in Heat Transfer* (Edited by C. A. Brebbia), Springer, New York, pp. 285-295.

Lesnic, D.; Elliott, L.; Ingham, D. B. (1996): Application of the boundary element method to inverse heat conduction problems. *International Journal of Heat and Mass Transfer*, vol. 39, pp. 1503-1517.

Lesnic, D.; Elliott, L.; Ingham, D. B. (1998): The solution of an inverse heat conduction problem subject to the specification of energies. *International Journal of Heat and Mass Transfer*, vol. 41, pp. 25-32.

Lin, S.-M.; Chen, C.-K.; Yang, Y.-T. (2004): A modified sequential approach for solving inverse heat conduction problems. *International Journal of Heat and Mass Transfer*, vol. 47, pp. 2669-2680.

Litkouhi, B.; Beck, J. V. (1986): Multinode unsteady surface element method with application to contact conductance problem. *Journal of Heat Transfer*, vol. 108, pp. 257-263.

Liu, C.-S. (2001): Cone of non-linear dynamical system and group preserving schemes. *International Journal of Non-Linear Mechanics*, vol. 36, pp. 1047-1068.

Liu, C.-S. (2004): Group preserving scheme for backward heat conduction problems. *International Journal of Heat and Mass Transfer*, vol. 47, pp. 2567-2576.

Liu, J.; Guerrier, B.; Benard, C. (1995): A sensitivity decomposition for the regularized solution of inverse heat conduction problems by wavelets. *Inverse Problems*, vol. 11 pp. 1177-1187.

Maz'ya, V.; Shaposhnikova, T. (1998): *Jacques Hadamard, A Universal Mathematician*. American Mathematical Society.

Monde, M.; Arima, H.; Liu, W.; Mitutake, Y.; Hammad, J. A. (2003): An analytical solution for two-dimensional inverse heat conduction problems using Laplace transform. *International Journal of Heat and Mass Transfer*, vol. 46, pp. 2135-2148.

Murio, D.A. (1989): The mollification method and the numerical solution of the inverse heat conduction problem by finite differences. *Computers and Mathematics with Applications*, vol. 10, pp. 1385-1396.

Murio, D. A.; Guo, L. (1990): A stable space marching finite differences algorithm for the inverse heat conduction problem with no initial filtering procedure. *Computers and Mathematics with Applications*, vol. 19, pp. 35-50.

Ochiai, Y.; Sladek, V. (2004): Numerical treatment of domain integrals without internal cells in three-dimensional BIEM formulations. *CMES: Computer Modeling in Engineering & Sciences*, vol. 6, pp. 525-535.

O'Mahoney, D. C. (2003): A differential quadrature solution of the two-dimensional inverse heat conduction problem. *International Communications in Heat and Mass Transfer*, vol. 30, pp. 1061-1070.

Palomo D. B., E. (2003): Multidimensional inverse heat conduction problems solution via Lagrange theory and model size reduction techniques. *Inverse Problems in Engineering*, vol. 11, pp. 515-539.

Pasquetti, R.; Le Niliot, C. (1991): Boundary element approach for inverse heat conduction problems: application to a bidimensional transient numerical experiment. *Numerical Heat Transfer*, vol. 20, pp. 169-189.

Prud'homme, M.; Nguyen, T. H. (1999): Fourier analysis of conjugate gradient method applied to inverse heat conduction problems. *International Journal of Heat and Mass Transfer*, vol.42, pp. 4447-4460.

Qiu, C.-Y.; Fu, C.-L.; Zhu, Y.-B. (2003): Wavelets and regularization of the sideways heat equation. *Computers and Mathematics with Applications*, vol. 46, pp. 821-829.

Reginska, T. (1995): Sideways heat equation and wavelets. *Journal of Computational and Applied Mathematics*, vol. 63, pp. 209-214.

Reginska, T.; Eldén, L. (1997): Solving the sideways heat equation by a wavelet-Galerkin method. *Inverse Problems*, vol. 13, pp. 1093-1106.

Reginska, T.; Eldén, L. (2000): Stability and convergence of a wavelet-Galerkin method for the sideways heat equation. *Journal of Inverse and Ill-Posed Problems*, vol. 8, pp. 31-49.

Reginska, T. (2001): Application of wavelet shrinkage to solving the sideways heat equation. *BIT*, vol. 41, pp. 1101-1110.

Reinhardt, H. J. (1991): A numerical method for the solution of two-dimensional inverse heat conduction problems. *International Journal for Numerical Methods in Engineering*, vol. 32, pp. 363-383.

Richtmyer, R. D.; Morton, K .W. (1967): *Difference Methods for Initial-Value Problems*. Second ed., Interscience Publishers, New York.

Seidman, T.; Eldén, L. (1990): An optimal filtering method for the sideways heat equation. *Inverse Problems*, vol. 6, pp. 681-696.

Shen, S.-Y. (1999): A numerical study of inverse heat conduction problems. *Computers and Mathematics with Applications*, vol. 38, pp. 173-188.

Shenefelt, J. R.; Luck, R.; Taylor, R. P.; Berry, J. T. (2002): Solution to inverse heat conduction problems employing singular value decomposition and model-reduction. *International Journal of Heat and Mass Transfer*, vol. 45, pp. 67-74.

Singh, K. M.; Tanaka, M. (2001): Dual reciprocity boundary element analysis of inverse heat conduction problems. *Computer Methods in Applied Mechanics and Engineering*, vol. 190, pp. 5283-5295.

Su, J.; Neto, A.J.S. (2001): Two-dimensional inverse heat conduction problem of sourse strength estimation in cylindrical rods. *Applied Mathematical Modelling*, vol. 25, pp. 861-872.

Taler, J.; Zima, W. (1999): Solution of inverse heat conduction problems using control volume approach. *International Journal of Heat and Mass Transfer*, vol. 42, pp. 1123-1140.

Videcoq, E.; Petit, D. (2001): Model reduction for the resolution of multidimensional inverse heat conduction problems. *International Journal of Heat and Mass Transfer*, vol. 44, pp. 1899-1911.

Wang, J.; Zabaras, N. (2004): A Bayesian inference approach to the inverse heat conduction problem. *International Journal of Heat and Mass Transfer*, vol. 47, pp. 3927-3941.

Wang, J.; Zabaras, N. (2005): Hierarchical Bayesian models for inverse problems in heat conduction. *Inverse Problems*, vol. 21, pp. 183-206.

Yang, C.-Y. (1999a): Estimation of the temperature-dependent thermal conductivity in inverse heat conduction problems. *Applied Mathematical Modelling*, vol. 23, pp. 469-478.

Yang, C.-Y. (1999b): The determination of two heat sources in an inverse heat conduction problem. *International Journal of Heat and Mass Transfer*, vol. 42, pp. 345-356.

Yuan, Y. (1993): *Application of the boundary element method to nonlinear and improperly posed problems*. PhD Dissertation, University of Leeds.